NANO LETTERS

Letter

Efficient Generation of Propagating Plasmons by Electron Beams

Wei Cai, Rebecca Sainidou, Jingjun Xu, A. Polman, and F. Javier Garci#a de Abajo

Nano Lett., **2009**, 9 (3), 1176-1181• DOI: 10.1021/nl803825n • Publication Date (Web): 19 February 2009

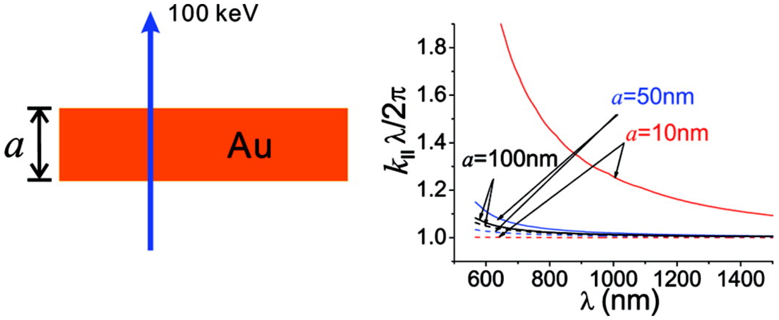

Nano Letters is published by the American Chemical Society. 1155 Sixteenth Street N.W., Washington, DC 20036

NANO
LETTERS

2009
Vol. 9, No. 3
1176-1181

Efficient Generation of Propagating Plasmons by Electron Beams

Wei Cai,[†,‡] Rebecca Sainidou,[†,§] Jingjun Xu,[‡] A. Polman,[||] and F. Javier García de Abajo[*,†]

Instituto de Óptica—CSIC, Serrano 121, 28006 Madrid, Spain, The Key Laboratory of Weak-Light Nonlinear Photonics, Ministry of Education and TEDA Applied Physics School, Nankai University, Tianjin 300457, China, Laboratoire d'Ondes et Milieux Complexes FRE CNRS 3102, Université du Havre, Place R. Schuman, 76610 Le Havre, France, and Center for Nanophotonics, FOM Institute AMOLF, Kruislaan 407, 1098 SJ Amsterdam, The Netherlands

Received December 18, 2008; Revised Manuscript Received February 2, 2009

ABSTRACT

We report highly efficient generation of propagating plasmons by electron beams in planar films, planar dielectric cavities, metallic wires, and nanoparticle waveguides. Electron-induced plasmon excitation is investigated in (1) gold thin films, both free-standing or supported on a silica substrate, (2) gold—silica—gold planar cavities, (3) gold nanowires, and (4) gold nanoparticle arrays. We obtain excitation yields as high as 10^{-2} plasmons per incoming electron over the visible and near-infrared range. Symmetric and antisymmetric plasmon modes are found to be more easily excited in thick and thin films, respectively, and in particular leaky plasmons in supported films are shown to be excited with very large probability exceeding one plasmon per electron. Generation of guided plasmons in metallic particle arrays is also proved to be attainable by aiming the electron at one end of the waveguide. The temporal evolution and spectral distribution of excited plasmons are discussed as well. Our results provide full support for the application of electron bombardment to excite propagating plasmons with high efficiency, thus solving the standing problem of plasmon generation at designated locations.

Propagating plasmons are becoming an essential ingredient in the design of optical devices at nanometer scales, in which the long propagation distances characterizing these excitations are combined with large confinement in the direction perpendicular to the metal surface.[1,2] Plasmon waveguiding has been experimentally demonstrated in a variety of systems, including planar metal films,[3−5] grooves patterned in metal surfaces,[6] surface-plasmon polariton (SPP) crystals,[7] and coupled nanoparticle arrays.[8,9] SPPs are actually a subject of increasing activity, with exciting results such as new designs capable of improving the compromise between propagation distances and lateral confinement, particularly in metallic wedges,[10] closely spaced wires,[11] and metallo-dielectric hybrid structures.[12]

The generation of SPPs at designated positions in a customizable fashion remains a standing problem in plasmonics. Recent studies have suggested that fast electrons provide a good solution to this problem by aiming an electron beam at the desired position on a metal surface, thus generating SPPs.[13−15] The generation of these plasmons has been monitored through the cathodoluminescence (CL) emission that they produce when SPPs are decoupled from the metal by a grating. Pioneering research on the use of CL to retrieve surface plasmon dispersion relations can be traced back to Ritchie *et al*.[16] and Heitmann,[17] followed by successful SPP dispersion mapping obtained from energy-loss and deflection-angle distributions of fast electrons traversing thin films.[18,19] More recently, the interference between directly generated light (transition radiation)[20,21] and SPPs outcoupled by a grating has been used to measure the SPP excitation yield in a planar surface.[22] Incidentally, CL has been employed to obtain snapshots of plasmons confined in metallic nanoparticles,[23−27] as well as standing waves of propagating plasmons in finite SPP resonant cavities,[28,29] while electron energy-loss spectroscopy (EELS) performed in thin samples can also reveal plasmon mode patterns with nanometer spatial resolution.[30,31]

In this paper, we discuss the generation of propagating plasmons in various systems, including free-standing and supported metallic thin films, metal—insulator—metal waveguides, metallic wires, and particle arrays. The plasmon excitation probability is calculated analytically for planar interfaces and using numerical methods for more complicated systems (nanowires and particle arrays). We quantitatively assess the plasmon

---

[*] Corresponding author, jga@cfmac.csic.es.
[†] Instituto de Óptica—CSIC.
[‡] The Key Laboratory of Weak-Light Nonlinear Photonics, Ministry of Education and TEDA Applied Physics School, Nankai University.
[§] Laboratoire d'Ondes et Milieux Complexes FRE CNRS 3102, Université du Havre.
[||] Center for Nanophotonics, FOM Institute AMOLF.

10.1021/nl803825n CCC: $40.75

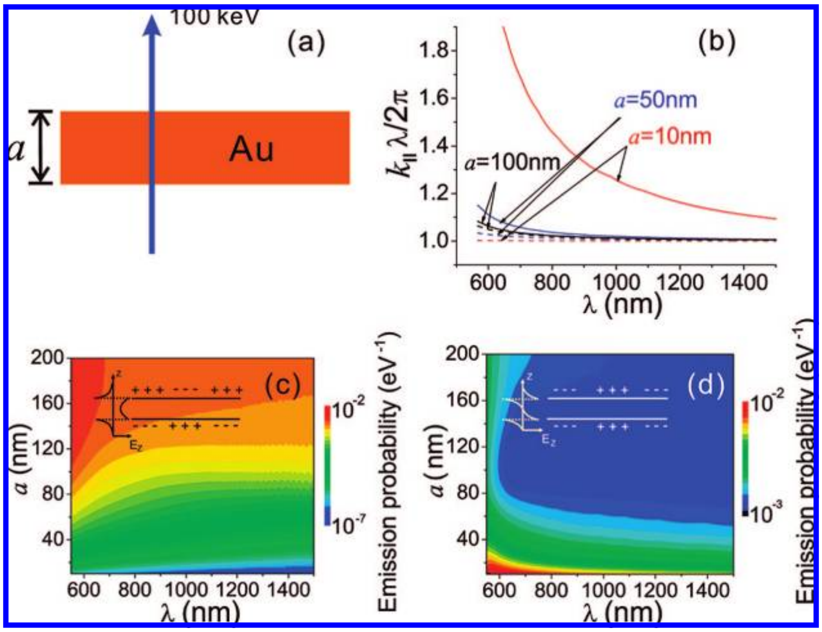

Figure 1. Plasmon generation in metallic thin films by an electron beam. (a) We consider a 100 keV electron traversing a free-standing gold thin film of thickness a. (b) Gold-film plasmon dispersion curves for thicknesses $a = 10$, 50, and 100 nm: parallel wavevector $k_{\|}$ versus vacuum wavelength λ. Symmetric and antisymmetric plasmon modes are represented by dashed and solid curves, respectively. (c, d) Probability that an electron creates a surface plasmon as a function of film thickness and vacuum wavelength. The probability is normalized per unit of plasmon energy range and it is separately given for symmetric (c) and antisymmetric (d) plasmon modes. The schematic insets in (c) and (d) show the induced charges (+ and − signs) and the normal electric field profile of these modes. Note the different color scales in (c) and (d).

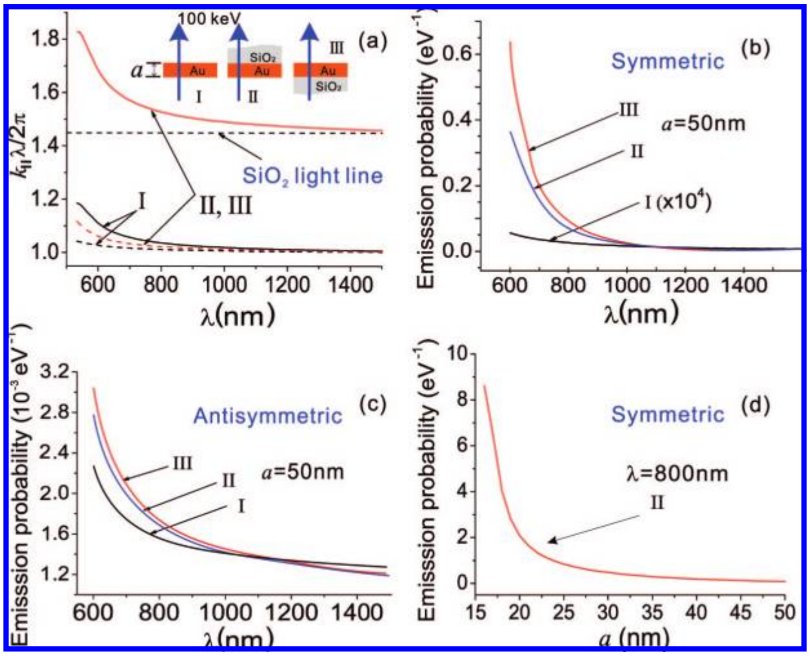

Figure 2. Plasmon generation in supported metal films. (a) Dispersion relation of plasmons in the structures I, II, and III, shown in the insets, for a gold thickness $a = 50$ nm. Symmetric and antisymmetric plasmon modes are represented by dashed and solid curves, respectively. (b, c) Probability of coupling to symmetric (b) and antisymmetric (c) plasmon modes in these structures. Note the different vertical scale in (c). The probability of curve I in (b) has been multiplied by a factor of 10^4. (d) Probability of exciting symmetric plasmon modes corresponding to a free-space wavelength of 800 nm in the structure II as a function of metal film thickness.

excitation yield in these systems and conclude that electron bombardment is a practical way of generating plasmons with high efficiency at positions controlled with nanometer precision through focused electron-beam bombardment.

We discuss first metal films and metal−insulator−metal (MIM) waveguides. Electron-beam excitation of plasmons in these systems can be studied by considering the electric field set up by an electron crossing two parallel interfaces with constant velocity v under normal incidence. We have worked out a quasi-analytical expression for the excitation probability that we use to obtain the results presented in Figures 1−3. The actual expression and its derivation are

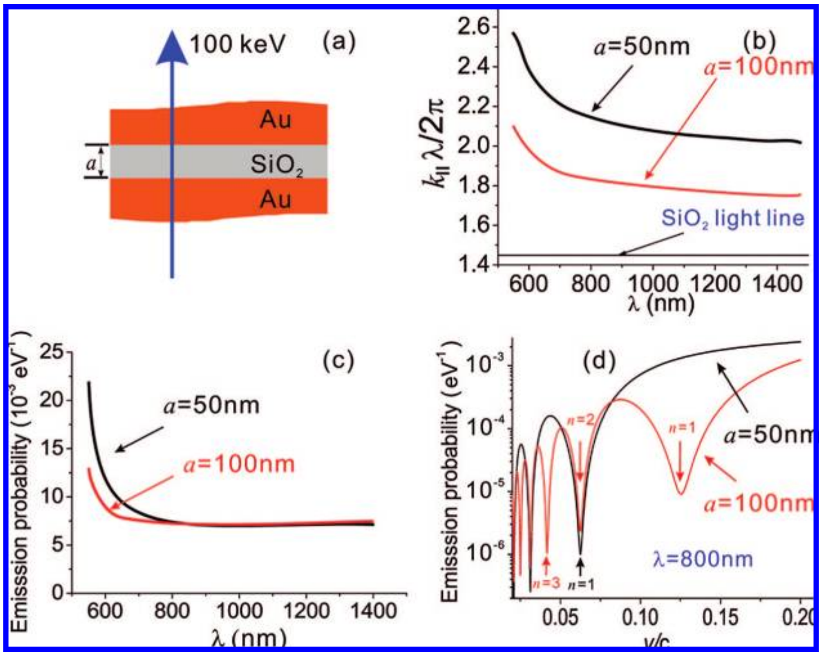

Figure 3. Plasmon generation in planar dielectric cavities. Only the symmetric plasmon mode is well-defined for the $a = 50-100$ nm cavities under consideration (b) (the antisymmetric mode is strongly attenuated). The plasmon generation probability per incoming electron and unit of plasmon energy range is given in (c) as a function of free-space wavelength for 100 keV electrons ($v = 0.55c$) and in (d) as a function of electron velocity for emission of plasmons corresponding to a free-space light wavelength of 800 nm. The arrows in (d) represent the predicted dip positions according to eq 1.

given in the Supporting Information. It is based upon a closed expansion of the electromagnetic field in the space of the parallel wavevector $\mathbf{k}_{\|}$ ($\perp \hat{\mathbf{z}}$) and frequency ω, so that the electric field is written as

$$\mathbf{E}(\mathbf{r},t) = \int \frac{d^2\mathbf{k}_{\|}\, d\omega}{(2\pi)^3} e^{i\mathbf{k}_{\|}\cdot(x,y) - i\omega t}\mathbf{E}(\mathbf{k}_{\|}, z, \omega)$$

The final expression for the probability (eq 2 in Supporting Information) is written for each plasmon mode n, defined by its dispersion relation $k_{\|} = k_{\|,n}$.

Figure 1 illustrates the excitation of SPPs in a free-standing gold film by 100 keV electrons (we take the dielectric function of gold from tabulated optical data).[32] Thin films have two types of SPP modes characterized by symmetric and antisymmetric distributions of both the normal electric field and the magnetic field across the film.[4,5,33] The former are less localized to the surface, as indicated by their parallel momentum, which is closer to the light cone $k_{\|} = k$. In the thin-film limit, the probability of exciting symmetric modes is very low because there is charge cancelation in the interaction of the electron with opposite induced charges associated to these modes on each side of the film[33] (see inset in Figure 1c). In contrast, charges contribute constructively in both sides for antisymmetric modes, to which the electron therefore couples strongly in thin films. For thick films, both symmetric and antisymmetric modes are excited with similar probability, which eventually converges to the probability for creating plasmons in a semi-infinite metal. The excitation yield exhibits a slow decrease with wavelength in all cases, so that the electron is acting as a relatively smooth supercontinuum plasmon source.

A gold film in an asymmetric environment presents an interesting scenario in which the symmetric plasmon branch becomes leaky, since it lies inside the light cone of the substrate.[5] Leaky modes are in fact infinitely delocalized, and one expects this to result in stronger coupling to the electron over an extended path length along its trajectory. This is actually the case, as shown in Figure 2 for gold films supported on silica (the dielectric function of silica is taken from ref 34 in this work). The excitation yield of leaky modes is several orders of magnitude larger compared to antisymmetric modes (cf. parts b and c of Figure 2). This strong coupling grows with decreasing metal film thickness, in accordance with the increasing degree of delocalization in that limit (Figure 2d), and because, unlike the symmetric environment situation, charge cancelation in the upper and lower interfaces is prevented by the breaking of symmetry produced by the substrate. The antisymmetric mode shows a similar trend of increasing excitation probability with decreasing metal film thickness similar to the free-standing film of Figure 1d.

Buried structures such as MIM cavities have attracted much interest in recent years due to their ability to produce extreme confinement[35] and effective negative index of refraction[36] of guided surface plasmons. Any excitation created in a MIM structure must be either absorbed by the metal or propagated as a cavity plasmon until it reaches its ends or is absorbed as well. The excitation yield takes values similar to that for the modes of the complementary metal film (cf. Figures 1c,d and 3c).

An interesting aspect of electron-induced plasmon excitation in MIM cavities is that the electron crosses a

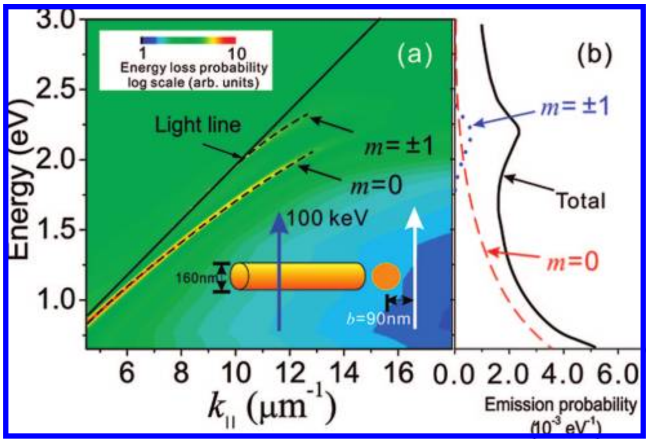

Figure 4. Coupling of an electron beam to metallic-wire plasmons. (a) Energy-loss probability of electrons passing at a distance of 10 nm from the surface of an infinitely long free-standing gold wire of 160 nm in diameter. The probability is decomposed into contributions arising from different values of the wavevector transfer along the wire axis $k_{||}$, according to eq 2. The probability exhibits maxima corresponding to excitation of plasmon modes with $m = 0, \pm 1$ azimuthal symmetry. The dispersion relation of $m = 0$ and $m = \pm 1$ guided plasmons is superimposed for comparison (dashed curves). (b) EELS probability integrated over parallel momentum (solid curve), and partial contributions of $m = 0$ and $m = \pm 1$ plasmon modes (dashed and dotted curves, respectively).

metal–insulator interface twice (on entrance to and exit from the cavity) with a delay determined by the ratio of the cavity width to the electron velocity, a/v. These two points of crossing act as localized sources of transition radiation[20,21] that can interfere with each other, thus producing oscillations of the symmetric-plasmon excitation yield with varying electron velocity (and also with varying angle of the trajectory for oblique incidence, which affects the noted delay as well). This prediction is fully confirmed by the calculations presented in Figure 3d, in which the dips are signaled by out-of-phase interference corresponding to the geometrical condition

$$\frac{(a/v)}{(\lambda/c)} = n \qquad (1)$$

where n is an integer. The dips predicted by this formula (arrows in Figure 3d) are remarkably close to the actual dips of the full calculation. Notice that n rather than $n + 1/2$ enters this equation, leading to dips corresponding to in-phase contributions from both interface crossings. This apparent contradiction stems from the fact that the polarization produced by the electron in the metal is opposite in direction for exit and entrance crossings, which explains the half-period term missing in the above formula (cf. the electron charge distribution for the symmetric mode in the inset of Figure 1c). Further support for this interpretation comes from the fact that a cavity of width $a = 50$ nm shows only half as many dips as a cavity with $a = 100$ nm (Figure 3d).

Fast electrons can also launch plasmons in laterally confined waveguides, for instance in a metallic wire.[25,26] We consider in Figure 4 the plasmon generation probability for an electron passing near an infinite gold wire of circular cross section and 160 nm in diameter. Plasmon excitation produces a relevant contribution to the electron energy loss. It is useful to consider the full EELS probability

$$\Gamma(\omega) = \int_0^\infty \mathrm{d}k_{||}\, \Gamma(k_{||}, \omega)$$

which we decompose here into contributions arising from different energy losses $\hbar\omega$ and wavevector components $k_{||}$ along the metal wire. This probability is obtained from the retarding force produced by the induced electric field acting back on the electron as[37]

$$\Gamma(k_{||}, \omega) = \frac{e}{\pi^2 \hbar\omega} \int \mathrm{d}t\, \mathrm{Re}\{\mathrm{e}^{-\mathrm{i}\omega t} \mathbf{v} \cdot \mathbf{E}^{\mathrm{ind}}(k_{||}, b, vt, \omega)\} \qquad (2)$$

where

$$E^{\mathrm{ind}}(k_{||}, b, vt, \omega) = \int \mathrm{d}x\, \mathrm{e}^{-\mathrm{i}k_{||}x} E^{\mathrm{ind}}(x, b, vt, \omega)$$

is the Fourier transform of the induced field along the direction x parallel to the wire, the electron trajectory is described by $z = vt$, and b is the *impact parameter* of the electron beam relative to the wire axis. $\Gamma(k_{||}, \omega)$ is directly related to the photonic local density of states in the vicinity of the wire.[38] Figure 4 shows that the electron is efficiently exciting plasmons with $m = 0$ symmetry (i.e., with $\exp(\mathrm{i}m\phi)$ dependence on the azimuthal angle ϕ). Also, $m = \pm 1$ modes are excited with smaller probability at higher energies as compared to the $m = 0$ modes. The plasmon-generation yield is shown in Figure 4b as obtained from the integral of $\Gamma(k_{||}, \omega)$ over $k_{||}$ in the region near the $m = 0$ (dashed curve) and $m = \pm 1$ (dotted curve) modes, and compared to the total loss probability (solid curve). Incidentally, these results are not very sensitive to the actual value of b, although grazing trajectories (b close to the radius) can provide the necessary large $k_{||}$ components to efficiently excite plasmons near the dispersion cutoff.

Coupling between plasmons in neighboring metallic particles has been the source of intense research for its application to waveguiding.[8,9,39] We discuss next the excitation of plasmon signals in particle arrays. Figure 5 represents the electric field produced by an electron passing near one end of 51 gold particles with a diameter of 160 nm spaced by a center-to-center distance of 165 nm. We obtain the induced electric field $E^{\mathrm{ind}}(x, \omega)$ from a multiple elastic scattering of multipolar expansions (MESME) formalism,[40] with converged results achieved after inclusion of multiples of orders $l \leq 12$. The field is strongly peaked near $\hbar\omega = 2$ eV (see Figure 5b), and it extends along the entire string (the total array length $\overline{AB}$ is 8.25 μm). It is instructive to examine the time evolution of the field (Figure 5c), which we obtain from the Fourier transform $E^{\mathrm{ind}}(x, t) = (2\pi)^{-1} \int \mathrm{d}\omega\, \exp(-\mathrm{i}\omega t) E^{\mathrm{ind}}(x, \omega)$. The electron interacts strongly with the string end as it passes nearby, but the induced field evolves along the string creating a pulse with central speed $\sim 0.75c$ (see dashed line in Figure 5c, drawn along the centroid of the pulse) in excellent agreement with the group velocity at the maximum intensity of the light dispersion curve (dashed curve in Figure 5d); although a wide spectral range of plasmons is excited, there is a preferred energy around 1.9 eV.

A similar analysis can be performed for nanowires of finite length (Figure 6). In particular, Figure 6b shows the propagation of the plasmon launched by the passing electron and successively reflected at the ends of a 160 nm diameter, 3 μm long gold wire (Figure 6c). Similar to the particle chain,

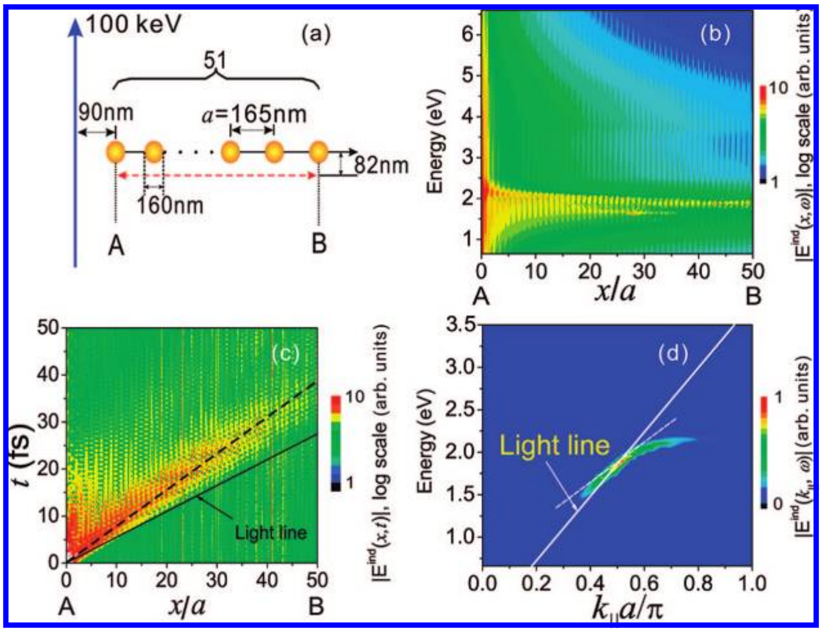

Figure 5. Electron-beam-induced plasmon generation in nanoparticle chains. (a) Scheme of the structure and geometry under consideration. (b) Induced electric field $E^{\mathrm{ind}}(x, \omega)$ (in frequency space ω) produced by the electron along the points of the $\overline{AB}$ segment (see red double arrow in (a)). (c) Same as (b), in the time domain: $E^{\mathrm{ind}}(x, t)$. (d) Fourier transform of $E^{\mathrm{ind}}(x, \omega)$ with respect to x, showing the dispersion relation of plasmons excited by the electron and propagating along the chain. The velocity of the launched pulse is found to be $\sim 0.75c$ (dashed line in (c)), in good agreement with the group velocity at the maximum of excitation probability along the guided-mode dispersion curve (dashed line in (d)).

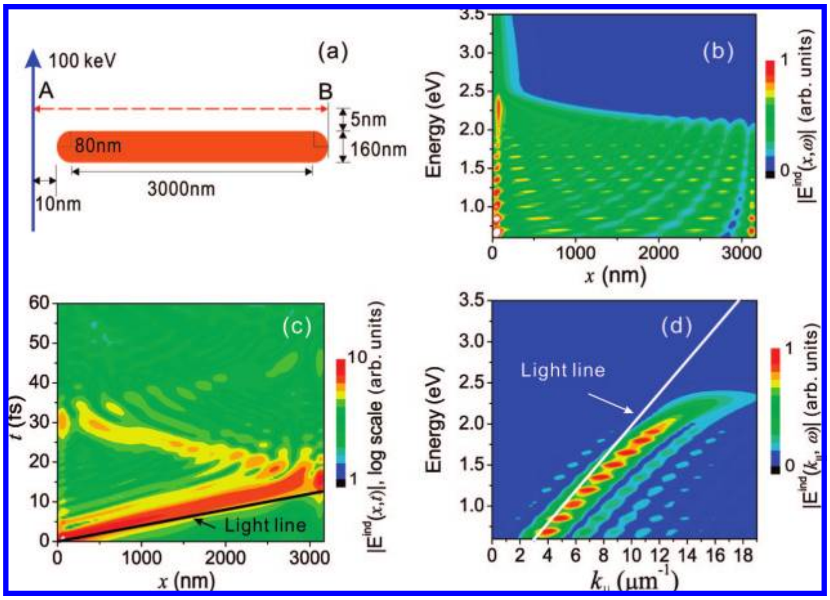

Figure 6. Temporal evolution of plasmons in finite nanowires. (a) Sketch of the geometry considered for excitation of nanowire plasmons by a 100 keV electron beam passing near one of the ends of a gold wire. (b) Induced electric field $E^{\mathrm{ind}}(x, \omega)$ (in frequency space ω) produced by the electron along the points of the $\overline{AB}$ segment (see red double arrow in (a)). (c) Same as (b), in the time domain: $E^{\mathrm{ind}}(x, t)$. (d) Fourier transform of $E^{\mathrm{ind}}(x, \omega)$ with respect to x, showing the dispersion relation of plasmons excited by the electron and propagating along the nanowire.

the plasmon wavepacket evolves with a distinct group velocity ($v \sim 0.8c$), but the propagation distance is much larger in this case, leading to standing waves that are best resolved in Figure 6b: see the intensity maxima that are aligned along horizontal lines in the plot, corresponding to the quantization condition $\Delta k_{\|} = \pi/L = 1.0\ \mu\mathrm{m}^{-1}$, where $L = 3160$ nm is the wire length. The same maxima show up in the dispersion relation of the $m = 0$ plasmon line in Figure 6d at equally spaced intervals in $k_{\|}$. The number of maxima along the rod increases with energy according to the same quantization condition. Modes with 4, 5,..., 11 antinodes are clearly discernible in Figure 6b. Furthermore, replicas of the plasmon mode dispersion can be observed in Figure 6d, separated by $\Delta k_{\|} \sim \pi/L$.

In conclusion, we have shown that fast electrons passing near nanostructured metals or crossing their boundaries can generate propagating surface plasmons with high efficiency. Electrons can be actually regarded as a source of evanescent optical fields that are ideally suited to couple to trapped modes such as plasmons, because those modes are also evanescent in the direction of confinement. These ideas are clearly illustrated in the generation of metallic-thin-film plasmons. In particular, the excitation of leaky plasmons in a metal film supported on an insulator leads to very intense leaky-plasmon emission, which eventually decays into light in the insulator, thus providing an efficient mechanism for supercontinuum light emission at subluminal velocities (i.e., at electron energies below the Cherenkov threshold in the insulator) assisted by the metal film. The efficient coupling between electron beams and SPPs is a universal phenomenon that can be exploited to generate plasmons in systems such as nanowires, particle arrays, and any other plasmon-supporting metal structures. We have followed the temporal evolution of the electron-generated plasmon pulses in particle arrays and nanorods of finite length, which move with principal velocity components that are well described by the plasmon group velocity, as calculated for infinitely long particle arrays and nanowires, respectively. In brief, our study reveals high yields of plasmon excitation by fast electrons, thus showing that electron bombardment constitutes a practical solution to the standing problem of plasmon generation at designated positions with high efficiency.

Acknowledgment. F.J.G.A. thanks Nikolay Zheludev and Martin Kuttge for many helpful and enjoyable discussions. This work has been supported by the Spanish MEC (MAT2007-66050 and Consolider NanoLight.es), the EU-FP6 (NMP4-2006-016881 "SPANS" and NMP4-SL-2008-213669 "ENSEMBLE"), the Chinese government (111 project No. B07013), and the FOM research program (supported by NWO).

Supporting Information Available: Analytical formalism for plasmon creation in thin films and buried planar cavities. This material is available free of charge via the Internet at http://pubs.acs.org.

References

(1) Barnes, W. L.; Dereux, A.; Ebbesen, T. W. *Nature* **2003**, *424*, 824–830.
(2) Zia, R.; Schuller, J. A.; Chandran, A.; Brongersma, M. L. *Mater. Today* **2006**, *9*, 20–27.
(3) Sarid, D. *Phys. Rev. Lett.* **1981**, *47*, 1927–1930.
(4) Berini, P. *Phys. Rev. B* **2000**, *61*, 10484–10503.
(5) Berini, P. *Phys. Rev. B* **2001**, *63*, 125417.
(6) Bozhevolnyi, S. I.; Volkov, V. S.; Devaux, E.; Laluet, J. Y.; Ebbesen, T. W. *Nature* **2006**, *440*, 508–511.
(7) Bozhevolnyi, S. I.; Erland, J.; Leosson, K.; Skovgaard, P. M. W.; Hvam, J. M. *Phys. Rev. Lett.* **2001**, *86*, 3008–3011.
(8) Quinten, M.; Leitner, A.; Krenn, J. R.; Aussenegg, F. R. *Opt. Lett.* **1998**, *23*1331–1333.
(9) Maier, S. A.; Kik, P. G.; Atwater, H. A.; Meltzer, S.; Harel, E.; Koel, B. E.; Requicha, A. A. G. *Nat. Mater.* **2003**, *2*, 229–232.
(10) Moreno, E.; Rodrigo, S. G.; Bozhevolnyi, S. I.; Martín-Moreno, L.; García-Vidal, F. J. *Phys. Rev. Lett.* **2008**, *100*, 023901.
(11) Manjavacas, A.; García de Abajo, F. J. *Nano Lett.* DOI 10.1021/nl802044t.
(12) Oulton, R. F.; Sorger, V. J.; Genov, D. A.; Pile, D. F. P.; Zhang, X. *Nat. Photonics* **2008**, *2*, 496–500.
(13) Bashevoy, M. V.; Jonsson, F.; Krasavin, A. V.; Zheludev, N. I.; Chen, Y.; Stockman, M. I. *Nano Lett.* **2006**, *6*, 1113–1115.
(14) van Wijngaarden, J. T.; Verhagen, E.; Polman, A.; Ross, C. E.; Lezec, H. J.; Atwater, H. A. *Appl. Phys. Lett.* **2006**, *88*, 221111.
(15) Peale, R. E.; Lopatiuk, O.; Cleary, J.; Santos, S.; Henderson, J.; Clark, D.; Chernyak, L.; Winningham, T. A.; Del Barco, E.; Heinrich, H.; Buchwald, W. R. *J. Opt. Soc. Am. B* **2008**, *25*, 1708–1713.
(16) Ritchie, R. H.; Ashley, J. C.; Emerson, L. C. *Phys. Rev.* **1964**, *135*, A759–A763.
(17) Heitmann, D. *J. Phys. C* **1977**, *10*, 397–405.
(18) Chen, C. H.; Silcox, J. *Phys. Rev. Lett.* **1975**, *35*, 390–393.
(19) Pettit, R. B.; Silcox, J.; Vincent, R. *Phys. Rev. B* **1975**, *11*, 3116–3123.
(20) Ginzburg, V. L.; Frank, I. M. *Zh. Eksp. Teor. Fiz. [Sov. Phys. JETP]* **1946**, *16*, 15–28.
(21) Landau, L. D.; Lifshitz, E. M.; Pitaevskii, L. P. *Electrodynamics of Continuous Media*; Pergamon Press: Oxford, 1984.
(22) Kuttge, M.; Vesseur, E. J. R.; Koenderink, A. F.; Lezec, H. J.; Atwater, H. A.; García de Abajo, F. J.; Polman, A. *Phys. Rev. B* **2009**, in press.
(23) Yamamoto, N.; Araya, K.; García de Abajo, F. J. *Phys. Rev. B* **2001**, *64*, 205419.
(24) Yamamoto, N.; Nakano, M.; Suzuki, T. *Surf. Interface Anal.* **2006**, *38*, 1725–1730.
(25) Vesseur, E. J. R.; de Waele, R.; Kuttge, M.; Polman, A. *Nano Lett.* **2007**, *7*, 2843–2846.
(26) Gómez-Medina, R.; Yamamoto, N.; Nakano, M.; García de Abajo, F. J. *New J. Phys.* **2008**, *10*, 105009.
(27) Bashevoy, M. V.; Jonsson, F.; MacDonald, K. F.; Chen, Y.; Zheludev, N. I. *Opt. Express* **2007**, *15*, 11313–11320.
(28) Hofmann, C. E.; Vesseur, E. J. R.; Sweatlock, L. A.; Lezec, H. J.; García de Abajo, F. J.; Polman, A.; Atwater, H. A. *Nano Lett.* **2007**, *7*, 3612–3617.
(29) Vesseur, E. J. R.; de Waele, R.; Lezec, H. J.; Atwater, H. A.; García de Abajo, F. J.; Polman, A. *Appl. Phys. Lett.* **2008**, *92*, 083110.
(30) Nelayah, J.; Kociak, M.; Stéphan, O.; García de Abajo, F. J.; Tencé, M.; Henrard, L.; Taverna, D.; Pastoriza-Santos, I.; Liz-Marzán, L. M.; Colliex, C. *Nat. Phys.* **2007**, *3*, 348–353.
(31) Bosman, M.; Keast, V. J.; Watanabe, M.; Maaroof, A. I.; Cortie, M. B. *Nanotechnology* **2007**, *18*, 165505.
(32) Johnson, P. B.; Christy, R. W. *Phys. Rev. B* **1972**, *6*, 4370–4379.
(33) Raether, H. *Surface Plasmons on Smooth and Rough Surfaces and on Gratings*; Springer Tracks in Modern Physics, 111; Springer-Verlag: Berlin, 1988.
(34) Palik, E. D. *Handbook of Optical Constants of Solids*; Academic Press: New York, 1985.
(35) Miyazaki, H. T.; Kurokawa, Y. *Phys. Rev. Lett.* **2006**, *96*, 097401.
(36) Lezec, H. J.; Dionne, J. A.; Atwater, H. A. *Science* **2007**, *316*, 430–432.
(37) Ritchie, R. H. *Phys. Rev.* **1957**, *106*, 874–881.
(38) García de Abajo, F. J.; Kociak, M. *Phys. Rev. Lett.* **2008**, *100*, 106804.
(39) Koenderink, A. F.; Polman, A. *Phys. Rev. B* **2006**, *74*, 033402. Koenderink, A. F.; de Waele, R.; Prangsma, J. C.; Polman A., *Phys. Rev. B* **2007**, *76*, 201403.
(40) García de Abajo, F. J. *Phys. Rev. Lett.* **1999**, *82*, 2776–2779. García de Abajo, F. J. *Phys. Rev. B* **1999**, *60*, 6103–6112.

NL803825N